Optica Applicata, Vol. XXXIX, No. 3, 2009

Two-dimensional numerical analysis on mid-infrared emission from IV-VI lead salt photonic crystal microcavity

SHAIBAL MUKHERJEE[1*], GANG BI[2**], JYOTI P. KAR[1], ZHISHENG SHI[1]

[1]School of Electrical and Computer Engineering, University of Oklahoma, Norman, Oklahoma-73019, USA

[2]School of Information Science and Electronic Engineering, Zhejiang University, City College, Hangzhou, Zhejiang-310027, China

[*]Corresponding author: shaibal@ou.edu

An optimal design of two dimensional (2D) hexagonal photonic bandgap (PBG) resonating micro-optical defect cavity on IV-VI lead salt material has been carried out. The nature of both the transverse electric (TE) and transverse magnetic (TM) band structure for the electromagnetic waves in the periodic triangular lattice pattern is formulated by the well-established plane wave expansion (PWE) method. The defect cavity is engineered to resonate at ~4.17 μm in TM bandgap. The field distribution in the defect cavity has been analyzed based on two very efficient and popular schemes – perturbation correction finite difference (FD) method and finite difference time domain (FDTD) mechanism which is truncated by uniaxial perfectly matched layer (UPML) absorbing boundary condition (ABC). FD method efficiently solves Helmholtz equations to evaluate the field distribution in the semiconducting waveguide for any single spectral wavelength. The numerical results by FD method are re-established by the FDTD scheme that incorporates a precise numerical analysis within a specified wavelength range.

Keywords: lead salts, plane wave expansion (PWE), finite difference (FD) perturbation method, finite difference time domain (FDTD), mid-infrared emission.

1. Introduction

The tremendous interest in mid-infrared spontaneous emission lies mainly in the fields of industrial trace-gas sensing application [1], environmental pollution control [2], and the inspection of industrial chemical processes. Mostly group III-V [3, 4] and IV-VI semiconductor materials [5–7] in the periodic table are pioneers in manufacturing mid-infrared light emitters to meet the application requirements. Easy spectral tunability of emitted light by joule-heating method, comparatively narrower full width

[**]The author is currently a visiting scholar at the University of Oklahoma.

half maximum (FWHM), and low power consumption make IV-VI materials a superior candidate to pursue the industry needs for gas sensors [8, 9] compared to its III-V counterparts. Other than a threshold population inversion a resonating cavity is essential for lasing to occur from semiconductor materials. The resonating cavity can be formed utilizing the natural cleavage planes of semiconductor. IV-VI lead salt materials have a natural cleavage plane along the [100] direction and therefore this is utilized to make Fabry–Perot resonating cavity for lasing at mid-infrared spectrum. We have theoretically [10] established that the molecular beam epitaxy (MBE) growth orientation along [110] direction is the best for lead salt laser fabrication as this orientation provides higher quantum efficiency and spectral gain [7]. Fabry–Perot resonating cavity formation can easily be formed by using {100} natural cleavage planes for [110] growth orientation as well. Recently we have demonstrated [11] electrically injected pulsed lasing at $\lambda = 5.2$ μm from lead salt epitaxial structure grown on a polished [110]-oriented PbSnSe substrate.

However, the MBE growth of lead salts is generally carried out on Si and BaF_2 substrates in order to reduce manufacturing cost as well as to avail of the established device fabrication technologies on these substrates. Both Si and BaF_2 have natural cleavage planes along [111] direction which is dissimilar to that of the epitaxial layer. The absence of {100} natural cleavage planes pose a serious challenge in device fabrication on these substrates.

This necessitates making a resonating cavity on the epitaxial layer by implementing the idea of well-known photonic crystal (PC) methodology, the physics of which does not depend on growth orientation. PC scheme demonstrates a perfect optical analogy of semiconductor bandgap where the electric potential distribution is governed by a periodicity of regularly distributed lattice dielectric medium (mainly air) in another highly contrasting dielectric medium. This helps in the confinement of light modes by creating a specific frequency bandgap which in other way opens up new horizons for tailoring the light-matter interaction in the crystal lattice. Due to the existence of bandgap effect in photonic crystals, optical waves corresponding to the bandgap frequency are forbidden [12] to propagate, whereas waves outside this range are allowed to propagate. This basically provides a provision for suitably engineering the crystal design and localizing light modes within a semiconductor slab. The size of the bandgap is determined by two factors: the dielectric contrast of the constituent materials that build up the photonic crystal and the higher dielectric material filling fraction [13]. Several research studies [14–18] regarding photonic crystal fabrication and characterizations in the semiconductor structure are cited in the literature. In this note, we investigate two-dimensional (2D) hexagonal PCs comprising of air columns periodically distributed on the PbSe-$Pb_{0.98}Sr_{0.02}Se$ multiple quantum well structure. The purpose of this study is to create a mid-infrared bandgap region in the photonic crystal and afterwards extracting the resonant mode in the frequency bandgap by designing a suitable defect cavity in the crystal structure. The resonant mid-infrared optical cavity mode thus obtained is immensely useful mainly for industrial trace gas sensing application.

The study of in-plane band structure behavior of the crystal is performed with the help of plane-wave expansion (PWE) method [19] by applying appropriate Bloch boundary conditions over a unit cell of the periodic photonic crystal. In order to choose an optimized design, the PC lattice is scanned to obtain modal band diagram by varying air-hole radius. Bandgap structure both for TE as well as TM polarizations for the optimized design is then evaluated. The resonating optical cavity is made by creating defects in the crystal structure which helps localize a mid-infrared optical mode in the bandgap region. The analysis of modal behavior of the defect cavity structure is accomplished by implementing two very popular mathematical schemes, namely finite difference (FD) perturbation method and finite difference time domain (FDTD) method. FD algorithm [20–23] along with the perturbation correction method [24, 25] which is a very popular method for optical waveguide analysis is devised to generate modal field distribution as well as effective refractive indices in the structure in a fast and accurate manner. The fundamental principle of the perturbation technique is to determine modal behavior of an imaginary structure, a "perturbed" form of the real waveguide structure. These values so obtained are then used as the initial parameters for the FD analysis of the real waveguide. The numerical simulation is continued by getting modal values of field and refractive indices from one convergence scan and using those as the initial parameters of the second scan till the analysis accurately reaches the desired mode within a specified tolerance. The results obtained by FD perturbation analysis are re-established by FDTD method. FDTD is a numerical tool that is implemented to find out discrete numerical solutions to the Helmholtz's electromagnetic equations for guiding waves in the photonic structure. The uniaxial perfectly matched layer (UPML) absorbing boundary condition (ABC) [26–28], which is a very efficient method of dealing with the scattering of particles in a vacuum, is implemented as the boundary layers outside the computational window.

2. Results and discussion

The PC semiconductor consists of PbSe-$Pb_{0.98}Sr_{0.02}Se$ multiple quantum well (MQW) structure, grown on BaF_2 substrate, which has arrays of dielectric air columns periodically distributed in hexagonal fashion on the surface (as shown in Fig. 1**a**). Figure 1**b** demonstrates the symmetry points of the first Brillouin zone in the periodic hexagonal crystal. The structure has the following constituent material parameters: refractive indices are $n_{\mathrm{PbSe}} = 5.0$ (bulk PbSe), $n_{\mathrm{PbSrSe}} = 4.6$ ($Pb_{0.98}Sr_{0.02}Se$) and $n_a = 1$ (air). Figure 1**c** is a schematic view of the MBE-grown epitaxial slab waveguide structure. The active region comprises of PbSe/PbSrSe MQW structure grown on Si(111) substrate with two top and bottom confinement layers. The active layer is considered to have a $\lambda/2$ thickness, where λ is the emission wavelength. In this case, the optical field along the vertical direction (*i.e.*, *y*-direction) could be successfully controlled by proper design of two confinement layers. In this report, we would consider only the two dimensional modal confinement of optical fields in the active region. In order to choose an optimized design, a scanning has been done to calculate

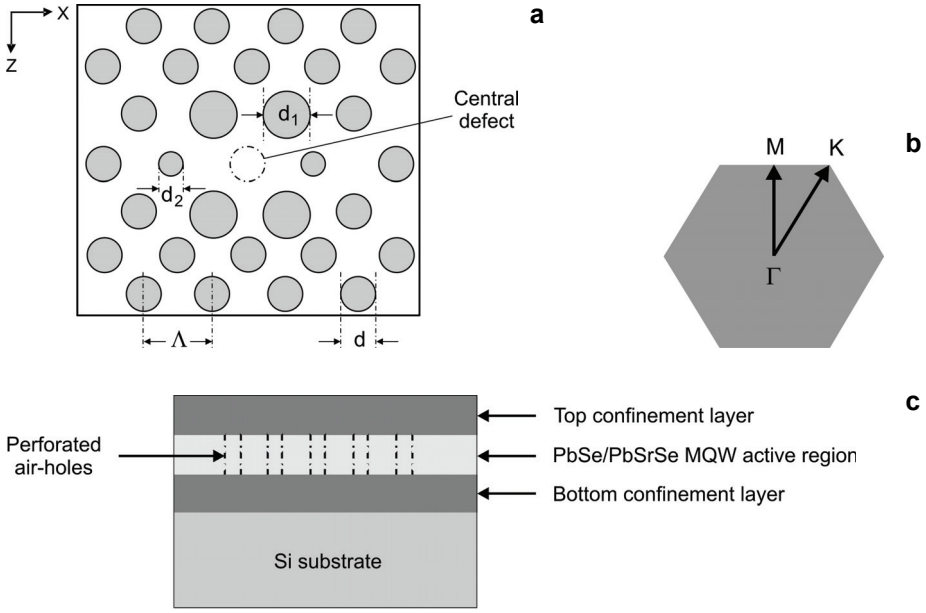

Fig. 1. Top view of triangular photonic crystal lattice structure (**a**). Schematic of the first Brillouin zone for the hexagonal lattice pattern (**b**). Schematic view of the MBE-grown sample with photonic crystal structure in the active region (**c**).

modal band structure and the corresponding bandgaps in the crystal lattice for varying radius of air-hole.

This is illustrated in Fig. 2, where all the frequency eigenvalues from the dispersion curves are combined along the single vertical line for each specific scanned value of radius. The crystal is optimally designed to have a diameter of dielectric air-hole (d) of 0.63 μm with a periodic lattice constant (Λ) of 0.96 μm. The air-fraction (d/Λ) in the photonic crystal plays an important role in creating bandgap. The band frequency tends to rise with an increase of air-fraction for a fixed lattice constant (Λ) in the crystal, as can be seen in Fig. 2**a**. In Figure 3, TE as well as TM band structures are plotted with the help of PWE method. However, it is worthwhile to mention that the resonating optical modes in such a periodically patterned crystal are not distinctively TE or TM but they can be thought of as TE-like and TM-like [29]. The band diagrams (for PC crystal with $d = 0.63$ μm, and $\Lambda = 0.96$ μm) in Fig. 3 demonstrate one narrow and another quite broad TM-like photonic bandgaps

T a b l e. TM bandgaps in the hexagonal periodic photonic lattice structure on IV-VI lead salt semiconductor.

Serial number	Bandgap [μm]
TM1	1.916–2.038
TM2	3.959–5.872

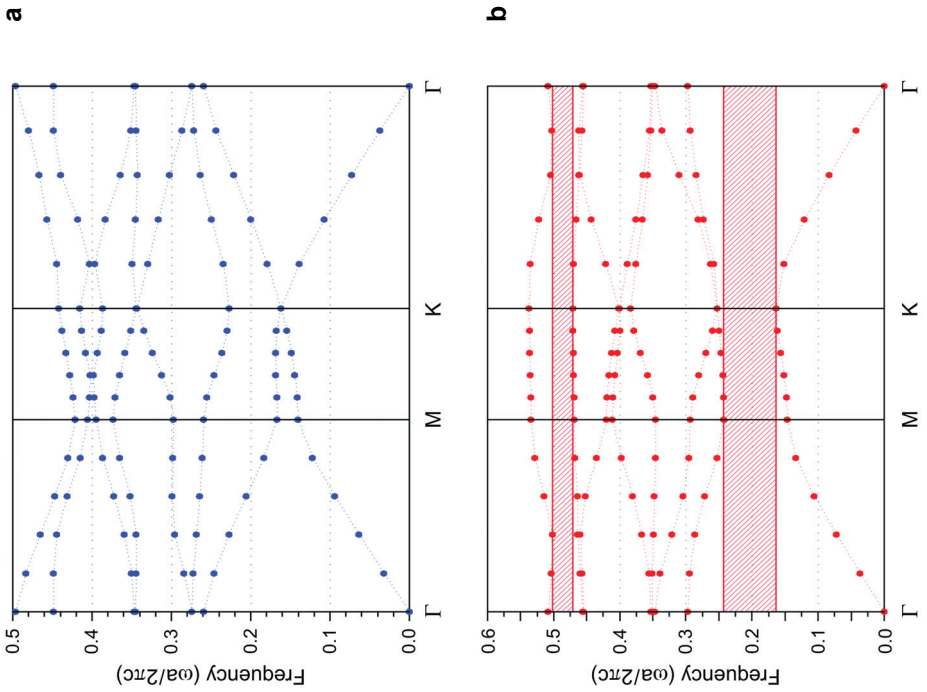

Fig. 3. Band structure of the photonic crystal for TE (**a**) and TM (**b**) polarized light.

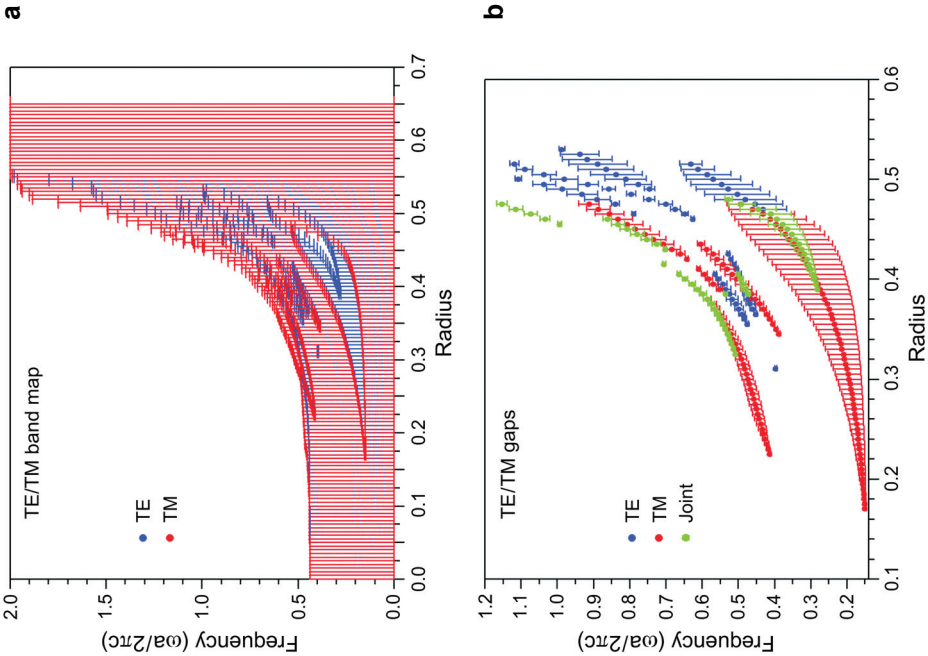

Fig. 2. Reduced band map for TE and TM modes (**a**), band map for TE, TM, and joint mode (**b**).

existing in the structure, but no TE-like bandgaps. The bandgap values are populated in the Table. Moreover, the broad TM bandgap covers the mid-infrared spectral region where room temperature photoluminescence from lead salts takes place. Therefore, we focus on engineering a defect cavity mode in this frequency bandgap region.

The defect cavity is designed (as illustrated in Fig. 1) by omitting the central air column, four vertical (two on top and two at bottom) lattice atoms along *X*-direction surrounding the central defect are made to have a diameter of 0.8 μm, two adjacent horizontal atoms along *Z*-direction surrounding the central defect are made to have a diameter of 0.46 μm.

At the first step, the properties of the localized defect cavity modes of the lattice structure such as propagation constant, effective refractive indices, electric field distribution are investigated with the help of FD perturbation algorithm. By applying the basic principles of finite difference discretizations [30], both single and double order differentials from electromagnetic Helmholtz equations guiding optical modes in the crystal lattice have been properly replaced. A computational window of a 800×800 mesh points for the periodic lattice is constructed along *X*-*Z* plane. The discretized electric field ($e_{p,\,r}$) at each mesh point in the computational domain is determined by:

$$e_{p,\,q} = \frac{e_{p,\,q+1} + e_{p,\,q-1} + e_{p+1,\,q} + e_{p-1,\,q}}{4 - (\Delta x)^2 k_0^2 \left(n_{p,\,q}^2 - n_{\text{eff}}^2 \right)} \tag{1}$$

where k_0 is the free space wave vector, $n_{p,\,q}$ is the refractive index at the computational point, and n_{eff} is the effective refractive index of the semiconductor material. A more precise value of modal effective refractive index (n_{effm}) is obtained after rigorous field converging scans and this is mathematically expressed as:

$$n_{\text{effm}}^2 = \frac{\int_{-\infty}^{\infty}\int_{-\infty}^{\infty} \left\{ (e_{p,\,q+1} + e_{p,\,q-1} + e_{p+1,\,q} + e_{p-1,\,q}) + \left[(\Delta x)^2 k_0^2 n_{p,\,q}^2 - 4 \right] e_{p,\,q} \right\} \mathrm{d}x\,\mathrm{d}z}{(\Delta x)^2 k_0^2 \int_{-\infty}^{\infty}\int_{-\infty}^{\infty} e_{p,\,q}^2\,\mathrm{d}x\,\mathrm{d}z} \tag{2}$$

Every time a value of n_{effm} is calculated following Eq. (2), the difference of this with that of the previous convergence value is evaluated until we reach a specified tolerance number in the modal effective refractive index difference. The resonating electric field distributions from the defect cavity in the photonic structure both for single as well as multi-modal conditions are depicted in Fig. 4.

FD perturbation technique determines the field distribution in the crystal at a fixed wavelength and therefore it proves to be time-consuming when determining the resonating wavelength for a specific optical cavity. Moreover, we needed to verify the numerical results with a time domain mathematical approach. This necessitates

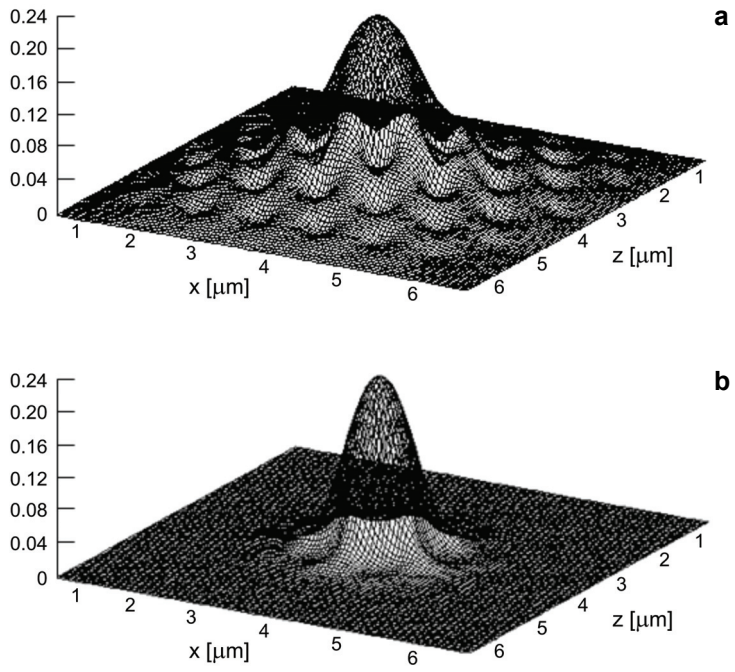

Fig. 4. Resonating electric field distribution at $\lambda = 4.17$ μm for multi-modal (**a**), and single modal (**b**) conditions.

the deployment of FDTD approach which produces a wideband response for the field distribution in the cavity by exciting the crystal with a Gaussian pulse.

The FDTD methodology is fundamentally based on numerical solutions to electromagnetic Helmholtz equations. FDTD together with the un-split PML ABC, which is implemented to truncate the boundary of the computational domain, have successfully demonstrated optical phenomenon like absorption and scattering [24]. The scheme is actually based on implementing Yee's numerical approach [31] to establish central difference approximations for both temporal and spatial derivatives. The space sampling for the calculation is done on a sub-micron scale. To ensure numerical stability of the mathematical calculation in the absorbing medium, we have utilized the Courant–Friedrichs–Levy (CFL) condition [32] as follows:

$$\Delta t \leq \frac{1}{c\sqrt{\dfrac{1}{(\Delta x)^2} + \dfrac{1}{(\Delta z)^2}}} \tag{3}$$

where Δx and Δz are the spatial steps along X- and Z-direction, respectively. The time step is designated by the integer n. Each mesh point in the computational zone has been assigned by the dielectric properties, namely permeability, permittivity, and

conductivity values of the host medium. The electric and magnetic field at each grid point is evaluated at half-time steps.

For 2D TE case in *X*-*Z* plane, electric and magnetic field components like E_y, H_x and H_z would exist. In the Cartesian coordinate system, these can be represented as:

$$E_y^n(p, q) = E_y^{n-1}(p, q) + \frac{\Delta t}{\varepsilon \Delta z}\left[H_x^{n-\frac{1}{2}}\left(p, q+\frac{1}{2}\right) - H_x^{n-\frac{1}{2}}\left(p, q-\frac{1}{2}\right)\right] + \\ - \frac{\Delta t}{\varepsilon \Delta x}\left[H_z^{n-\frac{1}{2}}\left(p+\frac{1}{2}, q\right) - H_z^{n-\frac{1}{2}}\left(p-\frac{1}{2}, q\right)\right]$$

$$H_x^{n+\frac{1}{2}}\left(p, q+\frac{1}{2}\right) = H_x^{n-\frac{1}{2}}\left(p, q+\frac{1}{2}\right) + \frac{\Delta t}{\mu_0 \Delta z}\left[E_y^n(p, q+1) - E_y^n(p, q)\right] \tag{4}$$

$$H_z^{n+\frac{1}{2}}\left(p+\frac{1}{2}, q\right) = H_x^{n-\frac{1}{2}}\left(p+\frac{1}{2}, q\right) - \frac{\Delta t}{\mu_0 \Delta x}\left[E_y^n(p+1, q) - E_y^n(p, q)\right]$$

Similar equations hold for H_y, E_x, and E_z in 2D TM case. In order to excite the photonic crystal structure, a Gaussian modulated continuous wave (GMCW) point source is considered which can be expressed as:

$$E_{\text{inc}} = A \exp\left[-\frac{0.5(t-t_0)^2}{T^2}\right] \sin(\omega t) \tag{5}$$

where A is the input wave amplitude, T is the half width, ω is the angular frequency, t_0 is the time offset. The rigorous numerical analysis produces a precise and efficient

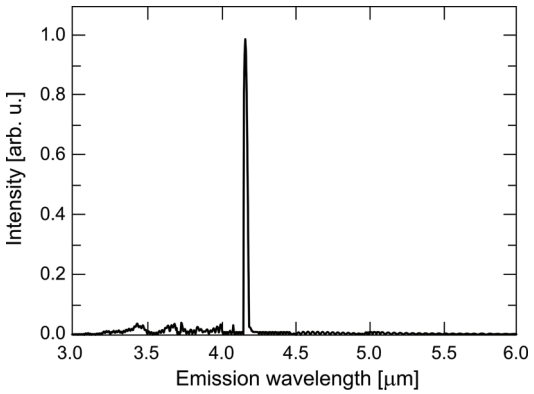

Fig. 5. Spectral response from DFT calculations after FDTD analysis of the resonating defect cavity.

time domain response for the field distribution in the defect cavity. To generate the spectral response corresponding to the time domain behavior, discrete Fourier transform (DFT) is applied. This calculates spectral response for a specific wavelength as shown by:

$$F(\omega) = \int_0^T F(t)\exp(-j\omega t)\mathrm{d}t = \sum_{n=0}^{N} F(n)\exp(-j\omega n\Delta t)\Delta t \tag{6}$$

where $F(n)$ is the time domain response, N is the number of time steps. The spectral field obtained from the defect cavity (as in Fig. 1) in the photonic crystal is seen to resonate at 4.17 μm and is plotted in Fig. 5.

The result seems to be in exact correlation with the numerical results obtained from the FD perturbation correction analysis. The optimized Q-factor for the resonating mode is calculated to be 5200.

3. Conclusions

We have demonstrated theoretical investigation of spontaneous mid-infrared emission from IV-VI semiconductor defect cavity in the hexagonal photonic crystal. The design is aimed to solve out problems of having resonating cavity for lead salt materials. The band structure calculations of the periodic crystal are performed using PWE method. Two approaches have been implemented to analyze and understand modal field distribution in the defect cavity. FD perturbation correction method and FDTD algorithms are very popular and well-established mathematical tools for optical waveguide analysis. It has been demonstrated that the FDTD results reasonably agree with that of FD perturbation method. A single TM-like mode working at 4.17 μm, having an optimized Q-factor of 5200, resonates in the designed defect cavity. The prospective practical applications of the single mid-infrared emission are mainly in industrial trace-gas sensing systems and emission monitoring.

Acknowledgements – Funding for this work was provided by the US DoD ARO under Grant W911NF-07-1-0587, DEPSCoR W911NF-04-1-0259, and from NSF EPS-0132534, DMR-0520550.

References

[1] FINDLAY P.C., PIDGEON C.R., KOTITSCHKE R., HOLLINGWORTH A., MURDIN B.N., LANGERAK C.J.G.M., VAN DER MEER A.F.G., CIESLA C.M., OSWALD J., HOMER A., SPRINGHOLZ G., BAUER G., *Auger recombination dynamics of lead salts under picosecond free-electron-laser excitation*, Physical Review B **58**(19), 1998, pp. 12908–12915.

[2] FEIT Z., MCDONALD M., WOODS R.J., ARCHAMBAULT V., MAK P., *Low threshold PbEuSeTe/PbTe separate confinement buried heterostructures diode lasers*, Applied Physics Letters **68**(6), 1996, pp. 738–740.

[3] EVANS A., YU J.S., SLIVKEN S., RAZEGHI M., *Continuous-wave operation of $\lambda \sim 4.8$ μm quantum-cascade lasers at room temperature*, Applied Physics Letters **85**(12), 2004, pp. 2166–2168.

[4] BEWLEY W.W., VURGAFTMAN I., KIM C.S., KIM M., CANEDY C.L., MEYER J.R., BRUNO J.D., TOWNER F.J., *Room-temperature "W" diode lasers emitting at* $\lambda \approx 4.0\ \mu m$, Applied Physics Letters **85**(23), 2004, pp. 5544–5546.
[5] PARTIN D.L., *Lead salt quantum effect structures*, IEEE Journal of Quantum Electronics **24**(8), 1988, pp. 1716–1726.
[6] SHI Z., XU G., MCCANN P.J., FANG X.M., DAI N., FELIX C.L., BEWLEY W.W., VURGAFTMAN I., MEYER J.R., *IV–VI compound midinfrared high-reflectivity mirrors and vertical-cavity surface-emitting lasers grown by molecular-beam epitaxy*, Applied Physics Letters **76**(25), 2000, pp. 3688–3690.
[7] SHI Z., LV X., ZHAO F., MAJUMDAR A., RAY D., SINGH R., YAN X.J., *[110] orientated lead salt midinfrared lasers*, Applied Physics Letters **85**(15), 2004, pp. 2999–3001.
[8] HOLLOWAY H., *Quantum efficiencies of thin-film IV–VI semiconductor photodiodes*, Journal of Applied Physics **50**(3), 1979, pp. 1386–1398.
[9] LOCKWOOD A.H., BALON J.R., CHIA P.S., RENDA F.J., *Two-color detector arrays by PbTe/* $Pb_{0.8}Sn_{0.2}Te$ *liquid phase epitaxy*, Infrared Physics **16**(5), 1976, pp. 509–514.
[10] XIAOLIANG LU, ZHISHENG SHI, *Theoretical investigations of [110] IV–VI lead salt edge-emitting lasers*, IEEE Journal of Quantum Electronics **41**(3), 2005, pp. 308–315.
[11] MUKHERJEE S., LI D., RAY D., ZHAO F., ELIZONDO S.L., JAIN S., MA J., SHI Z., *Fabrication of an electrically pumped lead-chalcogenide midinfrared laser on a [110] oriented PbSnSe substrate*, IEEE Photonics Technology Letters **20**(8), 2008, pp. 629–631.
[12] JOANNOPOULOS J.D., MEADE R.D., WINN J.N., *Photonic Crystals, Modeling the Flow of Light*, Princeton University Press, Princeton, N.J., 1995.
[13] JOANNOPOULOS J. D., VILLENEUVE P. R., FAN S., *Photonic crystals: putting a new twist on light*, Nature **386**(6621), 1997, pp. 143–149.
[14] KRAUSS T., SONG Y.P., THOMS S., WILKINSON C.D.W., DELARUE R.M., *Fabrication of 2-D photonic bandgap structures in GaAs/AlGaAs*, Electronics Letters **30**(17), 1994, pp. 1444–1446.
[15] KRAUSS T.F., DE LA RUE R.M., BRAND S., *Two-dimensional photonic-bandgap structures operating at near-infrared wavelengths*, Nature **383**(6602), 1996, pp. 699–702.
[16] O'BRIEN J., PAINTER O., LEE R., CHENG C.C., YARIV A., SCHERER A., *Lasers incorporating 2D photonic bandgap mirrors*, Electronics Letters **32**(24), 1996, pp. 2243–2244.
[17] BABA T., MATSUZAKI T., *Fabrication and photoluminescence of GaInAsP/InP 2-dimensional photonic crystals*, Japanese Journal of Applied Physics, Part 1 **35**(2B), 1996, pp. 1348–1352.
[18] HAMANO T., HIRAYAMA H., AOYYAGI Y., *Optical characterization of GaAs 2D photonic bandgap crystal fabricated by selective MOVPE*, [In] Conference on Lasers and Electro-Optics, Vol. 11 of 1997 OSA Technical Digest Series (Optical Society of America, Washington, D.C.), 1997, pp. 528–529.
[19] PLIHAL M., MARADUDIN A.A., *Photonic band structure of two-dimensional systems: the triangular lattice*, Physical Review B **44**(16), 1991, pp. 8565–8571.
[20] STERN M.S., *Rayleigh quotient solution of semivectorial field problems for optical waveguides with arbitrary index profiles*, IEE Proceedings, Part J, Optoelectronics **138**(3), 1991, pp. 185–190.
[21] BENSON T.M., KENDALL P.C., STERN M.S., QUINNEY D.A., *New results for waveguide propagation constants*, IEE Proceedings, Part J, Optoelectronics **136**(2), 1989, pp. 97–102.
[22] STERN M.S., *Semivectorial polarized finite difference method for optical waveguides with arbitrary index profiles*, IEE Proceedings, Part J, Optoelectronics **135**(1), 1988, pp. 56–63.
[23] GONTHIER F., LACROIX S., BURES J., *Numerical calculations of modes of optical waveguides with two-dimensional refractive index profiles by a field correction method*, Optical and Quantum Electronics **26**(3), 1994, pp. S135–S149.
[24] KUMAR A., VARSHNEY R.K., *Propagation characteristics of highly elliptical core optical waveguides: a perturbation approach*, Optical and Quantum Electronics **16**(4), 1984, pp. 349–354.
[25] KUMAR A., THYAGARAJAN K., GHATAK A.K., *Analysis of rectangular-core dielectric waveguides: an accurate perturbation approach*, Optics Letters **8**(1), 1983, pp. 63–65.

[26] BERENGER J.P., *A perfectly matched layer for the absorption of electromagnetic waves*, Journal of Computational Physics **114**(2), 1994, pp. 185–200.
[27] KATZ D.S., THIELE E.T., TAFLOVE A., *Validation and extension to three dimensions of the Berenger PML absorbing boundary condition for FD-TD meshes*, IEEE Microwave and Guided Wave Letters **4**(8), 1994, pp. 268–270.
[28] BERENGER J.P., *Three-dimensional perfectly matched layer for the absorption of electromagnetic waves*, Journal of Computational Physics **127**(2), 1996, pp. 363–379.
[29] PAINTER O., VUCKOVIC J., SCHERER A., *Defect modes of a two-dimensional photonic crystal in an optically thin dielectric slab*, Journal of the Optical Society of America B **16**(2), 1999, pp. 275–285.
[30] CHAUDHURI P.R., GHATAK A.K., PAL B.P., LU C., *Fast convergence and higher-order mode calculation of optical waveguides: perturbation method with finite difference algorithm*, Optics and Laser Technology **37**(1), 2005, pp. 61–67.
[31] KANE YEE, *Numerical solution of initial boundary value problems involving Maxwell's equations in isotropic media*, IEEE Transactions on Antennas and Propagation **14**(3), 1966, pp. 302–307.
[32] TAFLOVE A., BRODWIN M.E., *Numerical solution of steady-state electromagnetic scattering problems using the time-dependent Maxwell's equations*, IEEE Transactions on Microwave Theory and Techniques **23**(8), 1975, pp. 623–630.

Received November 14, 2008
in revised form January 23, 2009